Available online at www.sciencedirect.com

ScienceDirect

Ceramics International 35 (2009) 733–740

CERAMICS INTERNATIONAL

www.elsevier.com/locate/ceramint

$Pb(Zr_{0.95}Ti_{0.05})O_3$ powders and porous ceramics prepared by one-step pyrolysis process using non-aqueous Pechini method

Shaojun Qiu [a,*], Xiaodong Zheng [a], Chao Gao [a], Xiaoxian Gan [a], Jin Chen [b], Chen Yang [b], Huiqing Fan [b]

[a] *Xi'an Modern Chemistry Research Institute, Xi'an 710065, China*
[b] *State Key Laboratory of Solidification Processing, School of Materials Science and Engineering, Northwestern Polytechnical University, Xi'an 710072, China*

Received 25 June 2007; received in revised form 20 October 2007; accepted 6 February 2008
Available online 4 June 2008

Abstract

Using non-aqueous Pechini method, $Pb(Zr_{0.95}Ti_{0.05})O_3$ powders were prepared at low temperature by one-step pyrolysis process. The polymeric gels and powders were characterized using a range of techniques, such as DTG, XRD, SEM, Raman spectroscopy, and laser particle size distribution. The perovskite phase was formed at about 350–400 °C and some oxocarbonate impurities can be detected in all samples after calcining at 400–850 °C by one-step pyrolysis process. Phase pure and porous $Pb(Zr_{0.95}Ti_{0.05})O_3$ ceramics were obtained without pore formers from the powders by one-step pyrolysis process at 500 °C for 4 h. The relative densities were 87%, 91% and 94% for the ceramics sintered at 1100, 1150 and 1200 °C for 2 h, respectively. The porous ceramics sintered at 1200 °C for 2 h have homogeneously dispersed pores and fine-grain structures with an individual grain size of 0.7–2 μm.

Keywords: A. Powders: chemical preparation; B. Spectroscopy; B. Porosity; D. PZT

1. Introduction

Solid solutions of lead zirconate (PZ) and lead titanate (PT) in different proportions have found many important applications due to their piezoelectric and ferroelectric properties. In particular, the composite with a Zr:Ti molar ratio of 95:5, $Pb(Zr_{0.95}Ti_{0.05})O_3$ (PZT 95/5) is of great essence because of its great potential as a source of pulsed power for neutron generator through shock-wave compression [1,2].

The conventional way to prepare PZT is on the basis of the solid-state reaction among ZrO_2, PbO and TiO_2 at a significantly high processing temperatures (>1200 °C). Such high processing temperature would bring about several disadvantages: firstly, the overall procedure may not be under controllable and reproducible manner in some circumstances; secondly, the particle sizes are generally large (larger than 1 μm), with a broader size distribution; thirdly, impurities could be introduced in the ball milling and drying process which will affect the properties of the final product. Alternative approaches based on the wet chemistry, which can produce powders with homogeneous composition and size distribution, have been developed recently. The wet chemical methods include sol–gel, coprecipitation, hydrothermal synthesis and Pechini method [3–8]. For PZT 95/5 powders, the coprecipitation [9–11] and Pechini method [12] have been employed. One attractive character of the Pechini method is its lower operation temperature and hence the minimum possibility to phase segregation [8]. The objective of this method is the immobilization of metallic ions in a rigid polymer network. The metallic ions were dispersed in the polymer network at the atomic scale without precipitation and phase segregation. This process allows a complete control over the product stoichiometry, even for more complex oxide powders [13].

In the previous study [12], we have prepared PZT 95/5 powders by Pechini method in an aqueous solution. However, for some mixed oxides, there are a few insoluble metallic precursors. For the process of Pechini method, the presence of large amount

---

[*] Corresponding author at: Xi'an Modern Chemistry Research Institute, Xi'an 710065, China. Tel.: +86 29 88291839; fax: +86 29 88220423.
E-mail address: shaojqiu@yahoo.com (S. Qiu).

0272-8842/$34.00 © 2008 Elsevier Ltd and Techna Group S.r.l. All rights reserved.
doi:10.1016/j.ceramint.2008.02.001

of water would be unfavorable to the polymerization reaction of CA and EG, an equilibrium reaction.

$$\mathrm{R{-}OH} + \mathrm{R'COOH} \leftrightarrow \mathrm{R'COOR} + \mathrm{H_2O}$$

It could decrease the molecular weight of polyesters formed by CA and EG and we have presented the effect of the molecular weight of the polyesters on the evolution of phase behavior and morphology of the powders using aqueous Pechini method [12].

In this study, we present the experimental procedure using non-aqueous system from a simple Pechini method and introduce a one-step pyrolysis process at low temperature to synthesize well-crystallized PZT 95/5 powders. Furthermore, porous PZT 95/5 ceramics were synthesized from the chemically prepared powders without pore formers.

2. Experimental procedures

2.1. Sample preparation

Lead nitrate ($Pb(NO_3)_2$, ≥99.0%), zirconium oxynitrate ($ZrO(NO_3)_2 \cdot 2H_2O$, ≥99.0%) and titanium *n*-butoxide ($Ti(O\text{-}^nBu)_4$, ≥99.0%) were used as metallic cation sources. Citric acid (CA, AR) and ethylene glycol (EG, AR) were used as chelating agent. All chemicals were purchased from Sinopharm Chemical Reagent Co., Ltd., Shanghai, China.

PZT 95/5 powders and porous ceramics were prepared as summarized in Fig. 1. The molar ratio of EG:CA:Pb:Zr:Ti is 800:200:20:19:1. Initially, CA was transferred to the EG/Ti solution and stirred at 40 °C to get a clear solution and then kept stirring at 80 °C for another hour. Next, The metallic compounds were added until the system became transparent. Subsequently, the clear solution was heated to 140 °C and kept at this temperature for additional 2 h, to promote the polymerization of CA and EG. Whenever the polymerization occurs, the inorganic–organic hybrids became viscous accompanied with a color change from colorless to yellow. Finally, the gels were calcined by one-step pyrolysis process at 350–850 °C for 4 h in static air on an Al_2O_3 boat followed by natural furnace cooling to room temperature.

The powder was cold isostatically pressed at 100 MPa into disks and was sintered at 1100, 1150 and 1200 °C for 2 h in a sealed Al_2O_3 crucible with $PbZrO_3$ atmosphere powders.

2.2. Sample characterization

Derivative thermogravity (DTG) in air was performed on a TA TGA 2950 from 25 to 1000 °C at a heating rate of 20 °C min^{-1}, with an air flow rate of 200 mL min^{-1}. Fourier transform infrared spectrum (FTIR) in the range of 400–4000 cm^{-1} was recorded using KBr pellets on a Nicolet-60SXR-FTIR spectrometer with spectrum resolution of 4 cm^{-1}. A standard Raman spectrometer (Nicolet Almega Dispersive Raman) was used with the 532 nm line of an Nd:YV04 DPSS laser as an excitation source at a power level of 60 mW (40% of maximum power (150 mW)) and with a CCD (charge-coupled device) detector. Spectra were registered in the range from 100 to 2000 cm^{-1} at room temperature (18 °C). The powders and ceramics were characterized by X-ray diffractometry (XRD, X'Pert PRO MPD) to identify the various phases formed, using Cu Kα radiation (λ = 1.5406 Å) at 40 kV and 35 mA from 20° to 80° of 2θ. The average crystallite dimension was estimated from the most intense diffraction peak by means of the Scherrer equation. Scanning electron microscopy equipped with energy dispersive spectroscopy (EDS) was applied to obtain the microstructures of the powders (SEM, JEOL JSM-5800) and ceramics on fresh fracture faces (SEM, JEOL JSM-5610LV). Particle size distribution of the powders was measured by a laser-diffraction granularity tester (MASTERSIZER 2000). Prior to experiment, powders were ultrasonicated in water for 40 min. The densities of fired pieces were determined by the water displacement method.

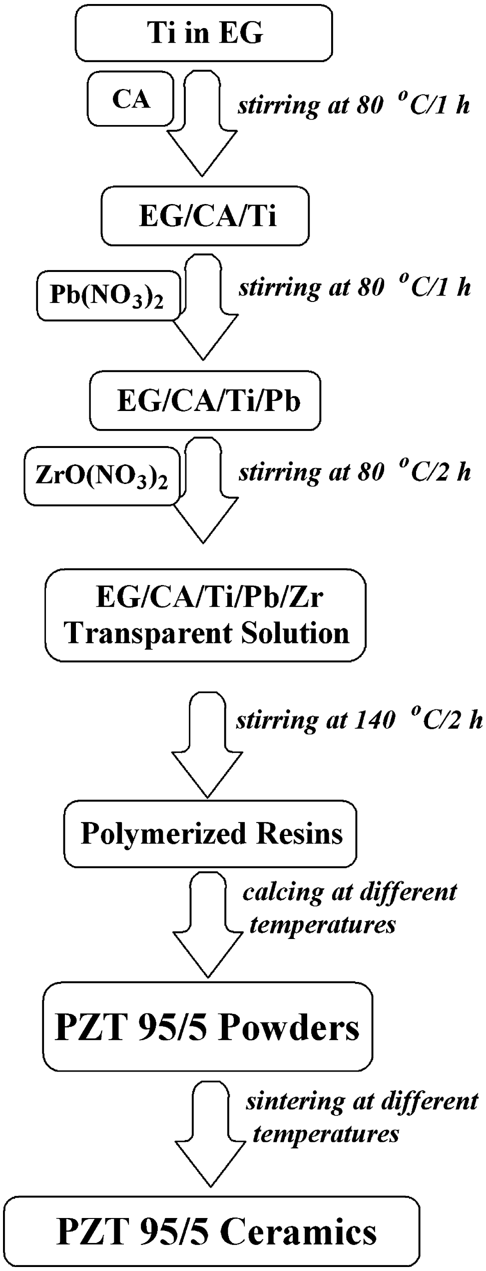

Fig. 1. Flowchart for the PZT 95/5 powders and ceramics.

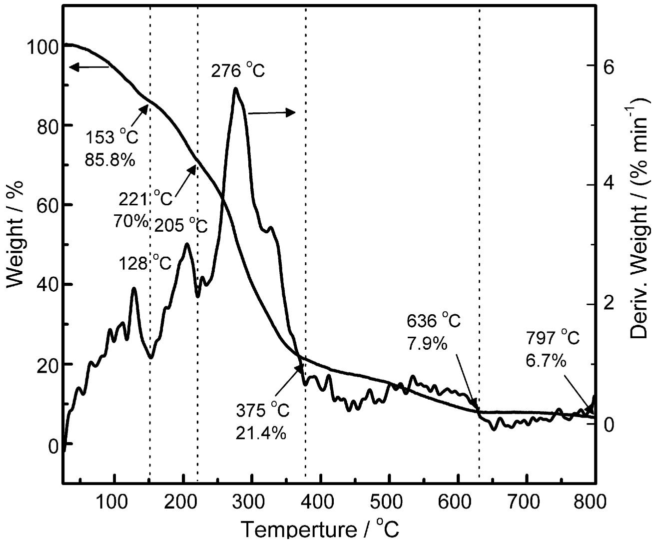

Fig. 2. DTG curve of polymeric gel. The dot line indicates the decomposition steps.

3. Results and discussions

3.1. DTG of gels

In the DTG experiment of the gels (Fig. 2), there are totally five weight loss steps in the temperature range of 25–800 °C. The first one appears in the temperature range of 25–153 °C with a weight loss of 14.2% and the corresponding temperature on DTG curve is at 128 °C. It could be most likely attributed to the elimination of water, formed during the condensation of CA and EG. The second step ranges from 153 to 221 °C, with a corresponding weight loss of 15.8% and a temperature of 205 °C on DTG curve. We attribute such process to the elimination of free EG (t_B(EG), 198 °C) entrapped in the gel. For the third one, a weight loss of 48.6% with a temperature range of 221–375 °C was observed and the transition temperature on DTG curve is at 276 °C. We attribute this procedure to the decomposition of the macromolecular chain, as formed by CA and EG. The macromolecular chain decomposes to some CA derived chelated cations and some small molecules such as CO_2, H_2O and other gases. Additionally, a few unreacted CA (with EG or metallic ions) decomposes in this stage. As suggested by Tsay and Fang [14], the fourth step in the temperature range of 375–636 °C with a weight loss of 13.5% could be attributed to the decomposition of the CA derived chelated cations, such as citraconic acid chelated structures. The perovskite phase PZT 95/5 powders are formed in this thermal process directly from some special CA-cations chelated structure without any intermediates. The highest decomposition happens in the temperature range of 636–797 °C, which is a slow process with a weight loss of 1.2%, indicating the complete elimination of organic matters in the powders. It should be mentioned that some carbonates still remain in the powders even though most organic compounds has been consumed (see later).

Noteworthy that the data obtained from DTG are deviated from the actual transition temperatures taking into account of the different decomposition conditions between DTG and the actual process. On the one hand, the amount of the gels used in the thermal analysis is small (about 1 mg), and thus thermal conduction is easier and therefore the decomposited products have little effect on the remaining gels (the gels could be coated by produced carbon in nature process). On the other, the flowed atmosphere takes the gas products from the system. Normally, the metallic ions are chelated by carboxyl group of free CA and partially polyesterized CA. The chelated structures would have special thermal properties. Unfortunately, we could not distinguish its contribution because the gels have a majority of organic matters.

3.2. One-step pyrolysis process

For Pechini method, the normal pyrolysis process includes a two-step thermal decomposition to obtain powders. At first, most of organic matters pyrolyze at a lower temperature, such as 300–500 °C, to obtain a polymeric precursor. Then, the polymer precursor calcines at a higher temperature, like 500–900 °C, to form a certain phase structure. The few remaining organic matters would decompose completely in the second step. In this study, we have utilized a one-step pyrolysis process to prepare PZT 95/5 powders, preventing the introduction of impurities and simultaneously making the overall process become power and time economic.

3.3. FTIR of gels and powders

Fig. 3 displays the FTIR spectra of the gels and the powders by one-step pyrolysis process under static atmosphere at 350–850 °C for 4 h. Four bands related to carboxylate stretching

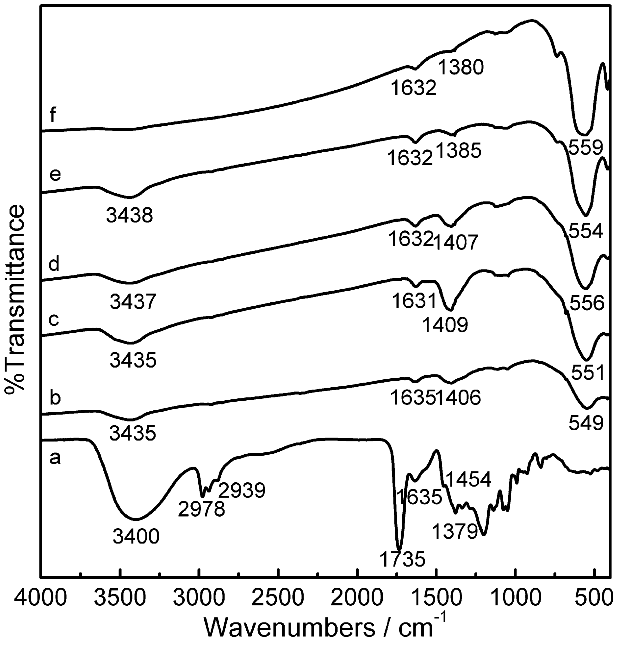

Fig. 3. FTIR of polymeric gels and PZT 95/5 powders by one-step pyrolysis process at different temperatures for 4 h. (a) Gels, (b) 350 °C, (c) 400 °C, (d) 500 °C, (e) 700 °C and (f) 850 °C, respectively.

modes at 1735, 1635, 1454 and 1379 cm^{-1} can be observed in the gels (Fig. 3(a)) [15,16]. The band at 1735 cm^{-1} could be assigned as the C=O stretching mode of the ester which was formed by polymerization of CA and EG. The 1635 and 1454 cm^{-1} bands could be assigned to asymmetric COO^- stretching mode for a unidentate complex and a bridging complex, respectively, formed from the chelation of CA and lead or zirconium ions. The 1379 cm^{-1} band could be assigned to symmetric COO^- stretching mode from the chelation of CA and lead or zirconium ions. The bands of 1635 and 1379 cm^{-1}, with $\Delta\nu = 256\ cm^{-1}$, suggest that the gels contain one unidentate group in the structure [17,18]. The other bands at 1500–850 cm^{-1} and 3500–2600 cm^{-1} are attributed to the polymeric network and OH, CH_2 and CH groups, respectively. The band at about 3435 cm^{-1} is attributed to the water adsorbed in the powders. The bands below 600 cm^{-1} are assigned to metal oxygen stretching mode from the chelation of CA and metallic ions.

When the gel is calcined at 350 °C for 4 h, the bands at 1380–1750 cm^{-1} disappear and two new bands occur at 1635 and 1406 cm^{-1}. The band at 1635 cm^{-1} is attributed to the COO^- stretching in unidentate metallic complex formed between CA and metal ions [16]. This band is still present in the powders even after calcination at 850 °C for 4 h, suggesting that the strong chelating ability provided by the α-hydroxylic acid groups of CA can stabilize different metal ions simultaneously within one molecule or complex [19]. The band at 1406 cm^{-1} is attributed to the carbonates derived from metallic-CA chelates as secondary phases. Decomposition of the precursor upon rapid heating yields an oxocarbonate compound and the crystal structure of the oxocarbonate is unknown [20]. As the calcined temperature increases, this band shifts to low wavenumber and the transmittance intensity of carbonates decreases. The lower temperature and inert atmosphere hinder the decomposition of carbonates [21]. The band at the range of 550–560 cm^{-1} is attributed to the absorption of PZT 95/5 structure.

FTIR results suggest that bonding between CA and the metallic ions begins to collapse below 350 °C and the derived carbonates are observed. Furthermore, it is important to note that the PZT 95/5 phase is detected even after calcined at lower temperatures, below 350 °C.

3.4. Raman of powders

Raman spectra of powders prepared by one-step pyrolysis process at 500 °C for 4 h are shown in Fig. 4, showing the PZT perovskite phase developed with tetragonal structure. The room temperature Raman spectrum contains all of the essential features of tetragonal polycrystalline solids prepared by conventional ceramic techniques. The peaks at wavenumber around 136.88, 206.38, 282.14, 336.14, 530.79 and 657.40 cm^{-1} are identified as $A_1(1TO)$, E(2TO), $B_1 + E$, $A_1(2TO)$, E(3TO) and $A_1(3TO)$, respectively. The other modes denoted in Fig. 6 are weak in comparison with the soft mode, and partially overlap with each other. All the Raman modes are assigned, according to the literature results [22–26].

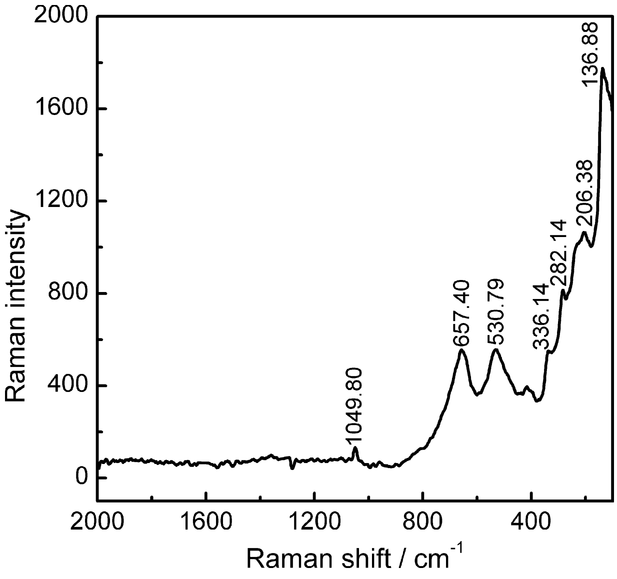

Fig. 4. Raman spectrum at room temperature for PZT 95/5 powders by one-step pyrolysis process at 500 °C for 4 h.

3.5. XRD of powders

To investigate the phase development with calcination temperatures, Fig. 5 shows XRD patterns of PZT 95/5 powders by one-step pyrolysis process at 400–850 °C for 4 h in static air.

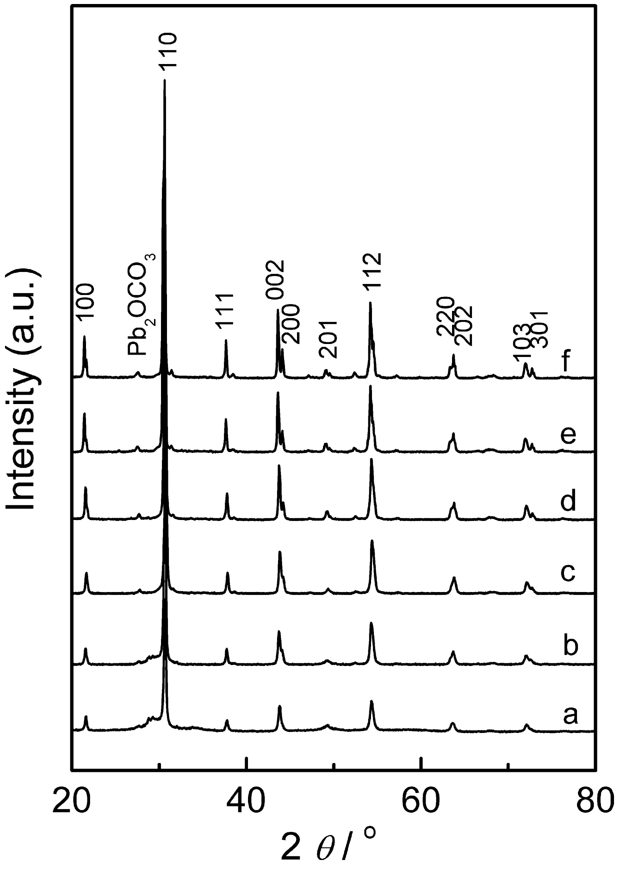

Fig. 5. XRD patterns of PZT 95/5 powders by one-step pyrolysis process at different temperatures for 4 h. (a) 400 °C, (b) 500 °C, (c) 600 °C, (d) 700 °C, (e) 800 °C and (f) 850 °C, respectively.

Table 1
The mean crystallite size from XRD results and size distribution parameter of PZT 95/5 powders calcined at different conditions by one-step pyrolysis process

	Calcination temperatures (°C)					
	400	500	600	700	800	850
Mean size (nm)	36	36	36	28	51	63
$D_{(50)}$ (μm)		4.305		2.021		5.768

It could be concluded that the perovskite phase of PZT 95/5 is predominant in the sample with some carbonates remained after calcination at 400 °C for 4 h, indicating incomplete decomposition of the gels to PZT 95/5 powders induced by the low temperature. Comparing with our previous results, the non-aqueous Pechini method in this study shows its advantage that more intense and sharper diffraction peaks of PZT 95/5 appear even for the powders calcined at 400 °C for 4 h [12]. To eliminate the secondary phase, higher calcination temperatures are applied using one-step pyrolysis process. The results (Fig. 5(b–f)) showed that the higher calcination temperature dose not reduce the amount of carbonates evidently. Blanco López et al. [21] have reported the complete elimination of $BaCO_3$ at 1000 °C was not sufficient.

By applying the Scherrer formula to the peak at about 30.7°, the mean crystallite sizes of PZT 95/5 powders are shown in Table 1. When the powders are obtained by one-step pyrolysis process at 400, 500 and 600 °C for 4 h, the calculated mean crystallite sizes are almost the same irrespective of calcination temperatures, which means the crystallite does not grow obviously in this temperature range. When the gels are applied at higher temperatures, there is a trough at 700 °C and then the calculated mean crystallite sizes increase while calcining at 800 and 850 °C. The decrease of mean crystallite sizes at 700 °C could result from the complete decomposition of the remained

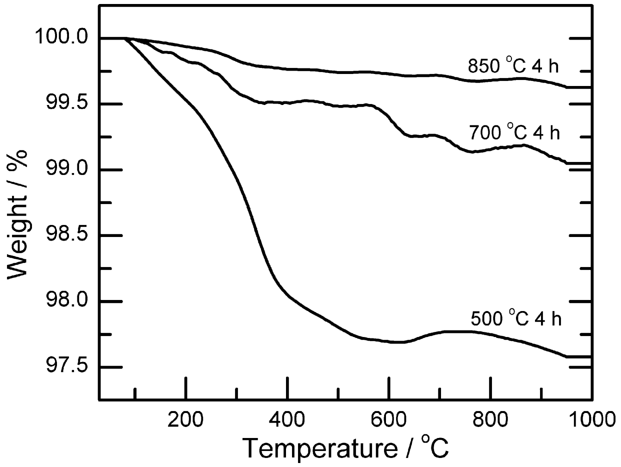

Fig. 6. DTG curves of PZT 95/5 powders by one-step pyrolysis process at different temperatures.

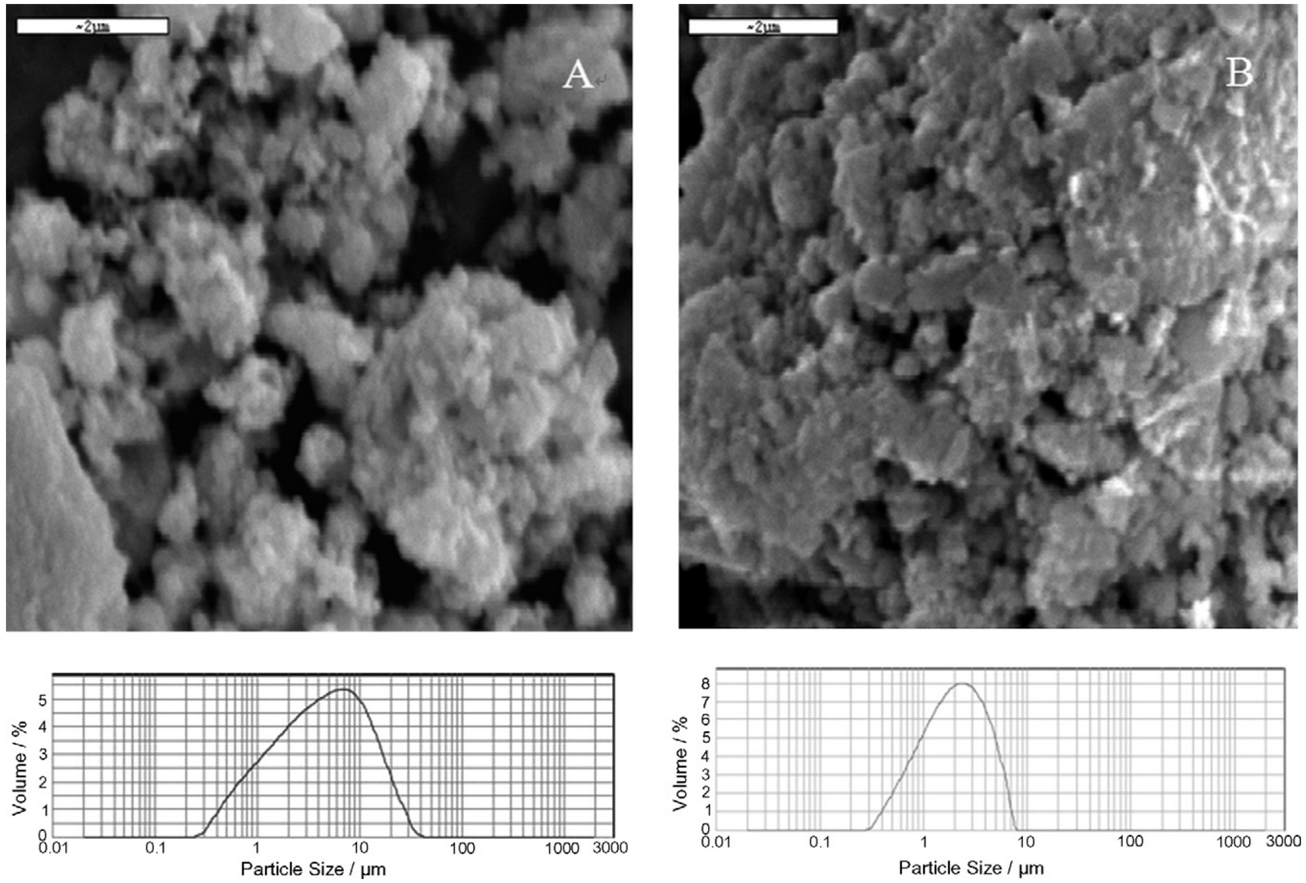

Fig. 7. SEM micrographs and size distribution of PZT 95/5 powders by one-step pyrolysis process at different temperatures for 4 h. (A) 500 °C, (B) 700 °C and (C) 850 °C, respectively. The scale bar in SEM is 2 μm.

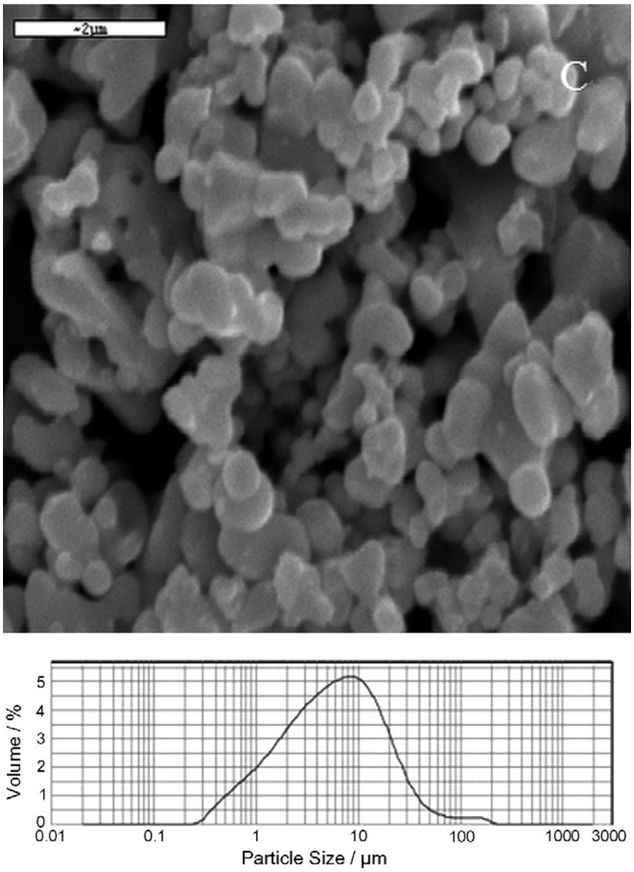

Fig. 7. (*Continued*).

organic matters (see later). Therefore, we could get small and well crystallized powders at 700 °C by one-step pyrolysis process.

3.6. DTG of powders

Fig. 6 shows the DTG curves of PZT 95/5 powders by one-step pyrolysis process at differnent temperatures. The rapid weight loss occurs before 400 °C which is attributed to the decomposition of the remained organic matters among the powders. In the temperature range of 30–1000 °C, the weight loss is 2.4%, 0.95% and 0.34% for powders calcined at 500, 700 and 850 °C for 4 h, respectively.

3.7. SEM and size distribution of powders

Microstructure and particle size distributions of PZT 95/5 powders calcined at 500, 700 and 850 °C for 4 h by one-step pyrolysis process are shown in Fig. 7. The tested values are listed in Table 1. Fig. 7 shows wide distribution of particle diameters. After calcination at 500 and 700 °C for 4 h, the powders are agglomeration composed of primary particles of particle size about 100 nm. When the gels calcined at 850 °C for 4 h, the powders are still agglomeration but the particle size increases to about 200–300 nm. It indicates that the powders have been partially sintered at this temperature. The order of particle size calcined at different conditions, $D_{(50)}$, corresponds with the calculated results from XRD well (Table 1).

3.8. Porous PZT 95/5 ceramics without additional pore formers

Dense PZT 95/5 materials possess low piezoelectric response and poor acoustic matching between the ceramics and the media (oxide–polymer composites) due to the great difference in density. Dungan and Storz [27] have demonstrated that additions of an external pore former, which results in porosity within the specimens, prevent high-voltage breakdowns at low temperature during explosive shock-wave transformation. Recently, decreases in the hydrostatic transformation pressure and increases in the range of pressure over which the transformation occurs for ceramics that are based on PZT 95/5, relative to increasing porosity, have been reported [28]. The change in transformation behavior was attributed to the enhanced magnitude and distribution of stress and strain in the vicinity of pores. The increased porosity could enhance the mechanical properties, hydrostatic piezoelectric voltage coefficient and hydrostatic figures of merit of ceramics [29]. Two types of pore formers, microcrystalline cellulose (MCC) rods and polymethyl methacrylate (PMMA) spheres, were added in varying amounts to adjust the final densities of the PZT 95/5 ceramics in literatures [27,29–31]. The pores sizes and distributions are strongly dependent on the species, amount and shape of the pore formers. However, there are only few studies on the control of pore size and distribution and the optimal density of the PZT 95/5 porous ceramics for neutron generator is still unclear.

In previous communication, we have presented the porous PZT 95/5 ceramics prepared by powders from aqueous Pechini method without additional pore formers [32]. Interestingly, porous ceramics having various densities could be obtained by

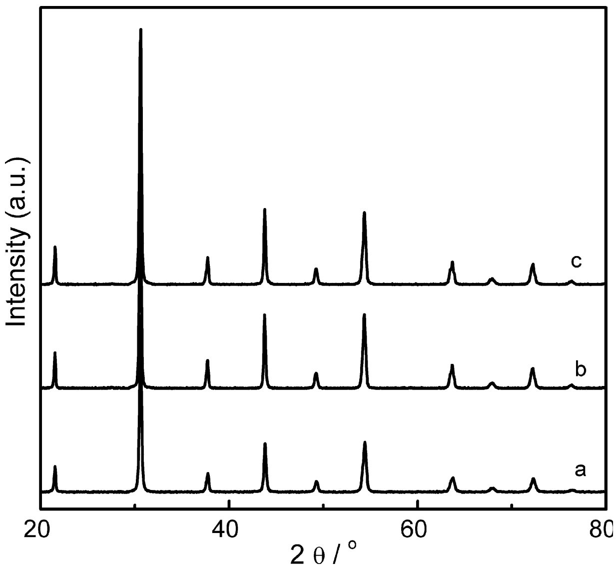

Fig. 8. XRD patterns of PZT 95/5 ceramics sintered for 2 h at different temperatures from one-step pyrolyzed powders calcined at 500 °C for 4 h. (a) 1100 °C, (b) 1150 °C and (c) 1200 °C, respectively.

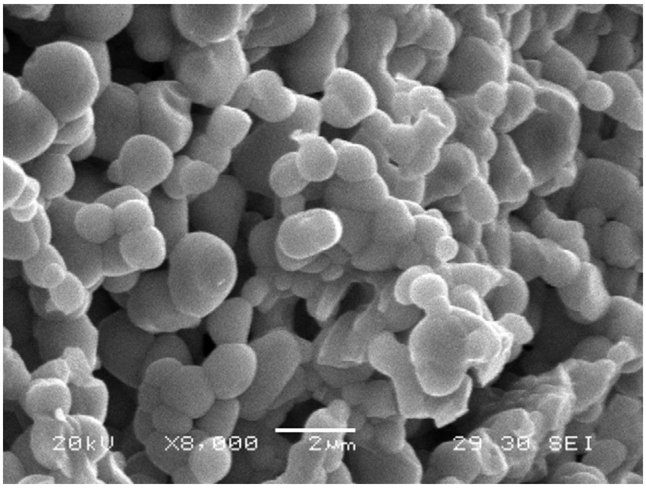

Fig. 9. SEM micrograph on a fresh fracture surface of PZT 95/5 ceramics sintered at 1150 °C for 2 h from one-step pyrolyzed powders calcined at 500 °C for 4 h. The scale bar in SEM is 2 μm.

sintering the powders at different temperatures. In the same way, the porous PZT 95/5 ceramics prepared by one-step pyrolysis process from non-aqueous Pechini method are examined in this study.

Fig. 8 shows the XRD results of ceramics sintered at different temperatures from powders calcined at 500 °C by one-step pyrolysis process. XRD patterns show complete perovskite structure of the ceramics sintered at 1100, 1150 and 1200 °C for 2 h. It is notable to see that the impurities in the powders by one-step pyrolysis process have been eliminated completely. The relative densities are 87%, 91% and 94% for the ceramics sintered at 1100, 1150 and 1200 °C for 2 h, respectively. One could conclude that the ceramics prepared from one-step pyrolyzed powders are porous structures. It could be attributed to the remaining organic matters among the one-step pyrolyzed powders. The decomposition of the remaining organic matters produces large amount of water vapor and carbon dioxide, and these gases escape from the green bodies forming pores in the ceramics [32]. When increasing the sintered temperatures, the formed pores shrink and the densities increase. The microstructure of the ceramic determined by SEM on a fresh fracture surface is presented in Fig. 9. For the porous PZT 95/5 ceramics from Pechini-type prepared powders without additional pore formers, the dark areas in SEM micrographs are pores and the pores are homogeneously dispersed. The sintered materials have fine-grain structures with individual grain of 0.7–2 μm in size.

Furthermore, for the powders by one-step pyrolysis process at 700 °C for 4 h, higher densities, i.e., 92%, 96% and 98% of relative densities, were obtained after sintered at 1100, 1150 and 1200 °C for 2 h, respectively. Turning back to Fig. 6, the powders calcined at 700 °C have less organic matters than that of powders calcined at 500 °C. When increasing calcining temperature for one-step pyrolysis process (>700 °C in this study), the prepared powders could behave similarly as sintering characters of powders from normal two-step pyrolysis step. More dense ceramics could be obtained from powders calcined at higher temperature.

4. Conclusions

PZT 95/5 powders were prepared by one-step pyrolysis process from non-aqueous Pechini method. The powders were characterized by XRD, DTG, FTIR and Raman spectra. The results indicate that the perovskite phase was formed at about 350–400 °C by one-step pyrolysis process. Though some oxocarbonate impurities can be detectable in the powders after calcination, pure PZT 95/5 ceramics were obtained after sintering the powders at 1100–1200 °C for 2 h. Additionally, porous ceramics could be obtained after thermal decomposition of the residue organics in the powders. The remarkable features of this kind of ceramics are the facile adjustment of their density by manipulation of the sintering temperatures and the possibility to prepare porous ceramic free from the addition of pore formers. In particular, the latter provides a convenient and attractive way to obtain homogeneous dispersed pores and fine-grain ceramics.

Acknowledgments

This work was supported by the fund of the State Key Laboratory of Solidification Processing in Northwestern Polytechnical University (NPU), China.

References

[1] D.G. Doran, Shock-wave compression of barium titanate and 95/5 lead zirconate titanate, J. Appl. Phys. 39 (1) (1968) 40–47.

[2] W.J. Halpin, Current from a shock-loaded short-circuited ferroelectric ceramic disk, J. Appl. Phys. 37 (1) (1966) 153–163.

[3] L.-W. Tai, P.A. Lessing, Modified resin-intermediate processing of perovskite powders. Part II. Processing for fine, nonagglomerated Sr-doped lanthanum chromite powders, J. Mater. Res. 7 (2) (1992) 511–519.

[4] L.-W. Tai, P.A. Lessing, Modified resin-intermediate processing of perovskite powders: Part I Optimization of polymeric precursors, J. Mater. Res. 7 (2) (1992) 502–510.

[5] P.A. Lessing, Mixed-cation oxide powders via polymeric precursors, Am. Ceram. Soc. Bull. 68 (5) (1989) 1002–1007.

[6] W.P. Guo, A.K. Datye, T.L. Ward, Synthesis of barium titanate powders by aerosol pyrolysis of a Pechini-type precursor solution, J. Mater. Chem. 15 (4) (2005) 470–477.

[7] M. Kakihana, T. Okubo, M. Arima, Y. Nakamura, M. Yashima, M. Yoshimura, Polymerized complex route to the synthesis of pure $SrTiO_3$ at reduced temperatures: implication for formation of Sr–Ti heterometallic citric acid complex, J. Sol–Gel Sci. Technol. 12 (2) (1998) 95–109.

[8] M.P. Pechini, Method of preparing lead and alkaline earth titanates and niobates and coating method using the same to form a capacitor, US patent 3,330,697 July 11, (1967).

[9] L. Guo, A. Lyashchenko, X.L. Dong, Synthesis of zirconium-rich PZT ceramics by hydroxide coprecipitation under hot-press, Mater. Lett. 56 (5) (2002) 849–855.

[10] J.A. Voigt, D.L. Sipola, B.A. Tuttle, M.T. Anderson, Nonaqueous solution synthesis process for preparing oxide powders of lead zirconate titanate and related materials, US patent 5,908,802 June 1, (1999).

[11] H. Yong, A. Lyashchenko, X.-L. Dong, C.-H. Luo, C.-L. Mao, S.-T. Chen, T. Zeng, Y.-L. Wang, Fabrication and properties of the Nb doped Zr-rich lead zirconate titanate ceramics by a heterogenous precipitation method, Ceram. Int. 33 (3) (2007) 497–503.

[12] S. Qiu, H. Fan, X. Zheng, $Pb(Zr_{0.95}Ti_{0.05})O_3$ powders synthesized by Pechini method: effect of molecular weight of polyester on the phase and morphology, J. Sol–Gel Sci. Technol. 42 (1) (2007) 21–26.

[13] M. Kakihana, Sol–gel preparation of high temperature superconducting oxides, J. Sol–Gel Sci. Technol. 6 (1) (1996) 7–55.

[14] J.-D. Tsay, T.-T. Fang, Effects of molar ratio of citric acid to cations and of pH value on the formation and thermal-decomposition behavior of barium titanium citrate, J. Am. Ceram. Soc. 82 (6) (1999) 1409–1415.

[15] A. Abreu, S.M. Zanetti, M.A.S. Oliveira, G.P. Thim, Effect of urea on lead zirconate titanate–$Pb(Zr_{0.52}Ti_{0.48})O_3$—nanopowders synthesized by the Pechini method, J. Eur. Ceram. Soc. 25 (5) (2005) 743–748.

[16] J.-D. Tsay, T.-T. Fang, T.A. Gubiotti, J.Y. Ying, Evolution of the formation of barium titanate in the citrate process: the effect of the pH and the molar ratio of barium ion and citric acid, J. Mater. Sci. 33 (16) (1998) 3721–3727.

[17] M. Kakihana, T. Nagumo, M. Okamoto, H. Kakihana, Coordination structure for uranyl carboxylate complexes in aqueous solution studied by IR and ^{13}C NMR spectra, J. Phys. Chem. 91 (24) (1987) 6128–6136.

[18] K. Nakamoto, Infrared and Raman Spectra of Inorganic and Coordination Compounds, 4th ed., Wiley, New York, 1986.

[19] M. Kakihana, M. Yoshimura, Synthesis and characteristics of complex multicomponent oxides prepared by polymer complex method, Bull. Chem. Soc. Jpn. 72 (7) (1999) 1427–1443.

[20] V. Petrykin, M. Kakihana, Chemistry and applications of polymeric gels precursors, in: S. Sakka (Ed.), Handbook of Sol–Gel Science and Technology. Processing, Characterization and Applications, Volume I Sol–Gel Processing, Kluwer Academic Publishers, 2005, pp. 77–103.

[21] M.C. Blanco López, G. Fourlaris, B. Rand, F.L. Riley, Characterization of barium titanate powders: barium carbonate identification, J. Am. Ceram. Soc. 82 (7) (1999) 1777–1786.

[22] G. Burns, B.A. Scott, Raman studies of underdamped soft modes in $PbTiO_3$, Phys. Rev. Lett. 25 (3) (1970) 167–170.

[23] G. Burns, B.A. Scott, Lattice modes in ferroelectric perovskites: $PbTiO_3$, Phys. Rev. B 7 (7) (1973) 3088–3101.

[24] J. Frantti, V. Lantto, Characterization of $Pb_{0.97}Nd_{0.02}(Zr_{0.55}Ti_{0.45})O_3$ thin-films prepared by pulsed-laser ablation, J. Appl. Phys. 76 (4) (1994) 2139–2143.

[25] J. Frantti, V. Lantto, J. Lappalainen, Symmetry consideration of Raman modes in Nd-doped lead zirconate titanate thin films for structure characterization, J. Appl. Phys. 79 (2) (1996) 1065–1072.

[26] F.M. Pontes, M.T. Escote, C.C. Escudeiro, E.R. Leite, E. Longo, A.J. Chiquito, P.S. Pizani, J.A. Varela, Characterization of $BaTi_{1-x}Zr_xO_3$ thin films obtained by a soft chemical spin-coating technique, J. Appl. Phys. 96 (8) (2004) 4386–4391.

[27] R.H. Dungan, L.J. Storz, Relation between chemical, mechanical, and electrical properties of Nb_2O_5-modified 95 mol% $PbZrO_3$–5 mol% $PbTiO_3$, J. Am. Ceram. Soc. 68 (10) (1985) 530–533.

[28] B.A. Tuttle, P. Yang, J.H. Gieske, J.A. Voigt, T.W. Scofield, D.H. Zeuch, W.R. Olson, Pressure-induced phase transformation of controlled-porosity $Pb(Zr_{0.95}Ti_{0.05})O_3$ ceramics, J. Am. Ceram. Soc. 84 (6) (2001) 1260–1264.

[29] T. Zeng, X.L. Dong, S.T. Chen, H. Yang, Processing and piezoelectric properties of porous PZT ceramics, Ceram. Int. 33 (3) (2007) 395–399.

[30] P. Yang, R.H. Moore, S.J. Lockwood, B.A. Tuttle, J.A. Voigt, T.W. Scofield, Chem-prep PZT 95/5 for neutron generator applications: the effect of pore forming agent type and density on the depoling behavior of chemically prepared PZT 95/5 ceramics, SAND2003–3866, 2003.

[31] R.E. Setchell, Shock wave compression of the ferroelectric ceramic $Pb_{0.99}(Zr_{0.95}Ti_{0.05})_{(0.98)}Nb_{0.02}O_3$: Hugoniot states and constitutive mechanical properties, J. Appl. Phys. 94 (1) (2003) 573–588.

[32] S. Qiu, H. Fan, C. Yang, J. Chen, Porous $Pb(Zr_{0.95}Ti_{0.05})O_3$ ceramics from chemically prepared powders without pore formers, J. Am. Ceram. Soc. 90 (10) (2007) 3293–3295.